ELSEVIER

Journal of Alloys and Compounds 388 (2005) 28–33

Journal of ALLOYS AND COMPOUNDS

www.elsevier.com/locate/jallcom

Antiferromagnetic order in $Ce_3Ni_{2+x}Si_{8-x}$ ($x \approx 1$)

V. Fritsch*, S. Bobev, J.D. Thompson, J.L. Sarrao

Los Alamos National Laboratory, Los Alamos, NM 87545, USA

Received 24 May 2004; received in revised form 7 July 2004; accepted 8 July 2004

Abstract

The structural, magnetic, thermodynamic and electrical properties of $Ce_3Ni_{2+x}Si_{8-x}$ ($x \approx 1$) were investigated by means of X-ray diffraction, magnetic susceptibility, specific heat and resistivity measurements. Structure determination by means of single-crystal X-ray diffraction, supported by elemental analysis revealed that $Ce_3Ni_{3.1(1)}Si_{6.9(1)}$ and its La-analogue $La_3Ni_{3.01(2)}Si_{6.99(2)}$ crystallize in the orthorhombic space group *Cmmm* (No. 65) with unit cell parameters of $a = 4.0935(4)$ Å, $b = 25.984(2)$ Å, $c = 4.1746(4)$ Å; and $a = 4.1257(3)$ Å, $b = 26.167(2)$ Å and $c = 4.2186(3)$ Å, respectively. The comprehensive property measurements performed on single crystals indicate the existence of an onset of antiferromagnetic order in $Ce_3Ni_{2+x}Si_{8-x}$ ($x \approx 1$) at $T_N = 4$ K and a Kondo-like resistivity with a Kondo temperature of $T^* = 75$ K. These results suggest a very light heavy-fermion behavior in the title compound with corresponding Sommerfeld-coefficient $\gamma = 51$ mJ/mol Ce K.

PACS: 71.27.+a; 75.40.Cx; 74.25.Fy; 74.25.Ha

Keywords: Magnetically ordered materials; Crystal growth; Crystal structure; Susceptibility; Heat capacity; Resistivity

1. Introduction

The 4f electrons of rare earth compounds reveal a variety of characteristics including heavy fermion behavior and magnetic order. A main goal of modern correlated electron physics is the search for new examples of these phenomena. Here, we report the result of one such search in the Ce–Ni–Si ternary phase diagram. Specifically we discuss the structure and the properties of $Ce_3Ni_{2+x}Si_{8-x}$ ($x \approx 1$), which has been previously known as $Ce_3Ni_2Si_8$ [1]. This compound and its isostructural $La_3Ni_{2+x}Si_{8-x}$ crystallize in an orthorhombic structure with the space group *Cmmm* [1], and a schematic drawing of this structure is shown in Fig. 1. Structure determination by means of single-crystal X-ray diffraction revealed a disorder between Ni and Si on one of the crystallographic sites, resulting in actual compositions of $Ce_3Ni_{3.1(1)}Si_{6.9(1)}$ and $La_3Ni_{3.01(2)}Si_{6.99(2)}$. The latter were confirmed by elemental analysis on single crystals and therefore, $Ce_3Ni_{2+x}Si_{8-x}$ and $La_3Ni_{2+x}Si_{8-x}$ ($x \approx 1$) will be denoted as $Ce_3Ni_3Si_7$ and $La_3Ni_3Si_7$ hereafter.

2. Synthesis

All manipulations were performed under vacuum or in an inert atmosphere. The starting materials were pure elements—La (ingot, Ames 99.9%), Ce (ingot, Ames 99.9%), Ni (pieces, Alfa 99.9%), Si (lump, Alfa 99.9999%), Ga (lump, Alfa 99.99%), and Sn (shot, Alfa 99.99%) and they were used as received. La or Ce, Ni and Si with the desired stoichiometric ratios were first arc-melted in an evacuated and back-filled with high purity Ar arc-melter over a copper hearth. The buttons were flipped and arc-melted several times in order to assure homogeneity. These arc-melted products were then crushed and loaded with a 50-fold excess of low-melting Ga or Sn, which serve as a crystal growth media for the title compounds.

$Ce_3Ni_3Si_7$ and $La_3Ni_3Si_7$ were initially identified as the major products of reactions set up with the intention to produce $Ce_3Ni_4Si_{13}$ and $La_3Ni_4Si_{13}$, Si-based analogs of the Remeika phases ($Pr_3Rh_4Sn_{13}$-type, Pearson's code *cP*40). For that purpose, stoichiometric mixtures of the elements in ratios 3:4:13 were arc-melted as described above. The powder patterns of the arc-melted products indicated that these were mixtures of

* Corresponding author: Tel.: +1-505-665-7036; fax: +1-505-665-7652.
E-mail address: fritsch@lanl.gov (V. Fritsch).

0925-8388/$ – see front matter © 2004 Elsevier B.V. All rights reserved.
doi:10.1016/j.jallcom.2004.07.007

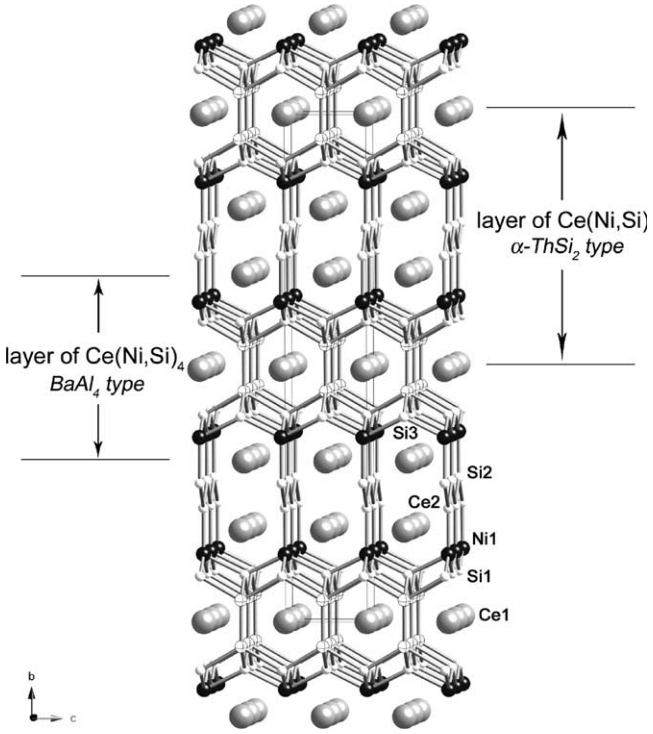

Fig. 1. Ball and stick representation of the crystal structure of $Ce_3Ni_3Si_7$, viewed along the direction of *a*-axis. The crossed circles represent the disordered Si/Ni positions.

polycrystalline $Ce_3Ni_3Si_7$ or $La_3Ni_3Si_7$, unreacted Si and Ni.

To obtain single crystals from these materials, the polycrystalline arc-melted mixtures were annealed with Ga and Sn. The crystal growth reactions were carried out in 5 cm^3 alumina crucibles, which were then put in fused silica ampoules. These, in turn, were closed under vacuum by flame sealing. Further and more elaborate details on the flux-growth synthetic procedures can be found elsewhere [2]. Reactions were carried out in a programmable Lindberg muffle furnace using the following temperature profile: quick ramping (250 °C/h) to 1100 °C, dwell at that temperature for 24 h, followed by cooling (−5 °C/h) to 850 °C, dwell at that temperature for 48 h, and subsequent cooling (−5 °C/h) to 650 °C. At that point, the molten Ga (or Sn) was removed by centrifugation. It was found that Ga is a better media for growth of $Ce_3Ni_3Si_7$, while Sn is a superior flux for growing crystals of $La_3Ni_3Si_7$. Plate-like crystals with silver-metallic luster, some of them very large (up to ca. 8–10 mm) were isolated and used for the structure determination work and for the physical properties measurements. Both materials are stable in air and moisture, but slowly dissolve in mineral acids.

3. Single crystal X-ray diffraction

Intensity data for both $Ce_3Ni_3Si_7$ and $La_3Ni_3Si_7$ were collected at 90(3) K on a Bruker SMART 1000 CCD diffractometer equipped with a low-temperature apparatus. A hemisphere of data was collected using graphite monochromatized Mo Kα radiation (0.3° *ω*-scans, $2\theta_{max} \approx 63°$) for (1) a crystal of $Ce_3Ni_3Si_7$ (0.20 mm × 0.13 mm × 0.10 mm; $T_{min}/T_{max} = 0.0955/0.2154$, 979 total reflections, 403 unique reflections, $R_{int} = 2.39\%$); and (2) a crystal of $La_3Ni_3Si_7$ (0.09 mm × 0.05 mm × 0.04 mm; $T_{min}/T_{max} = 0.2577/0.4918$, 2143 total reflections, 465 unique reflections, $R_{int} = 3.70\%$). Intensity data were collected using the SMART software [3] and were subsequently corrected for Lorentz and polarization effects and integrated in Laue symmetry *mmm* with the aim of the SAINT package [4]. Empirical absorption correction was applied with the SADABS software package [5]. Data were subsequently refined on F^2 (data to parameter ratio greater than 13) with the aid of the SHELXTL V5.10 package [6]. All atoms are refined with anisotropic displacement parameters with scattering factors and absorption coefficients [7]. Data revealed that the $La_3Ni_3Si_7$ single crystal was of higher quality and better diffracting than the crystal of $Ce_3Ni_3Si_7$, in which the mosaicity was considerably worse. Therefore, the following discussion on the structure is based entirely on the data from $La_3Ni_3Si_7$. Further details of the data collection and structure refinement, as well as positional and equivalent isotropic displacement parameters for $La_3Ni_3Si_7$ are given in Tables 1 and 2.

The unit cell parameters for $La_3Ni_3Si_7$ ($a \approx 4.1$ Å, $b \approx 25.9$ Å, $c \approx 4.2$ Å), especially the very short *a* and *c* axes were closely examined by taking long exposure frames on the SMART and were confirmed. The reflection conditions for the observed reflections clearly confirmed the C-centering and established only three possible space groups—the chiral *C*222 (No. 21), the non-centrosymmetric *Cmm*2 (No. 35), and the centrosymmetric *Cmmm* (No. 65). The latter *Cmmm* was chosen based on intensity statistics calculations and relevant figure of merit, and the structure of $La_3Ni_3Si_7$ was subsequently solved by direct methods and refined to convergence.

Table 1
Selected data collection and refinement parameters for $La_3Ni_3Si_7$

Empirical formula	$La_3Ni_{3.01(2)}Si_{6.99(2)}$	$Ce_3Ni_{3.1(1)}Si_{6.9(1)}$
Formula weight	789.5	796.18
Space group, Z	*Cmmm* (No. 65), 2	
Radiation, λ (Å)	Mo Kα, 0.71073	
Temperature (K)	90(3)	
Unit cell parameters		
a (Å)	4.1257(3)	4.0935(4)
b (Å)	26.167(2)	25.984(2)
c (Å)	4.2186(3)	4.1746(4)
V (Å^3)	455.43(6)	444.03(7)
μ (cm^{-1})	206.75	223.44
ρ_{calc} (g/cm^3)	5.757	5.955
R_1/wR_2[a]	2.83/6.38	5.50/12.80

[a] $R_1 = \sum ||F_o| - |F_c|| / \sum |F_o|$; $wR_2 = (\sum[w(F_o^2 - F_c^2)^2] / \sum[w(F_o^2)^2])^{1/2}$, where: $w = 1/[\sigma^2 F_o^2 + (A \cdot P) + B \cdot P]$; *A* and *B* are weight coefficients, $P = (F_o^2 + 2F_c^2)/3$.

Table 2
Atomic coordinates and equivalent isotropic displacement parameters (U_{eq}) for $La_3Ni_3Si_7$. U_{eq} is defined as one-third of the trace of the orthogonalized U_{ij} tensor

Atom	Site	x	y	z	U_{eq}
La1	2a	0	0	0	0.004(1)
La2	4j	0	0.3165(1)	1/2	0.004(1)
Ni1	4i	0	0.1333(1)	0	0.004(1)
Si1	4i	0	0.4075(1)	0	0.007(1)
Si2	4i	0	0.2240(1)	0	0.005(1)
Si3	4j	0	0.0933(1)	1/2	0.007(1)
M4[a]	4j	0	0.4542(1)	1/2	0.010(1)

[a] M4 is refined as a statistically distributed Si and Ni in ratio of 49.5(8):50.5(8).

Subsequently, it was realized that this structure type has long been known and adopted by at least one other rare-earth nickel silicide, $Ce_3Ni_2Si_8$ (Pearson's code *oC*26, *Cmmm*, $a = 4.085(2)$ Å, $b = 25.9558(8)$ Å, $c = 4.1786(9)$ Å) [1]. However, careful examination of the published structure revealed that at least one temperature factor was implausible, providing even stronger motivation to study this somewhat uncommon structure type. Hence, the unit cell axes and the nomenclature for the atomic positions were assigned accordingly (Table 1), as the $Ce_3Ni_2Si_8$-type was adopted for the initial structural model.

During initial refinement cycles, all atoms were refined with isotropic atomic displacement parameters (*U*'s hereafter). The refinement yielded somewhat poor R_1 and wR_2 factors, 6.87 and 30.24%, respectively, and it did not converge. In the difference Fourier map there was a residual peak of approximately 20.5 $e^-/Å^3$ at one of the Si atoms Si4—the same Si position in the original report that had negative *U*. This suggests that there is extra electron density on that site and implies the possibility for a heavier atom (e.g. Ni) to occupy it. Thus, Si and Ni were simultaneously refined with site occupancy constrained to unity. R_1 and wR_2 factors dropped to 3.87 and 12.47%, respectively. Convergence was easily achieved and there were virtually no residual peaks in the difference Fourier map (the highest peak was approximately 3.3 $e^-/Å^3$). This indicates that there is a statistical distribution of Si and Ni at this site (previously assigned as occupied by Si only, but with the reported implausible *U*), and the refined composition of La:Ni:Si = 3:3:7 (Table 1) is in excellent agreement with microprobe analysis (below).

In the final refinement, all six crystallographically independent sites (two La, one Ni, three Si, and one mixed Si/Ni) were refined with anisotropic atomic displacement parameters. The final R_1 and wR_2 factors of 2.83 and 6.38%, respectively, as well as a goodness-of-fit indicator of 1.112 (based on 369 F^2's ($F^2 > 2\sigma_{F^2}$) and 30 refined parameters) attest to the good quality of the single crystal and the correctness of the structure determination. Further details of the crystal structure investigations may be obtained from the Fachinformationszentrum Karlsruhe, 76344 Eggenstein–Leopoldshafen, Germany (fax: +49 7247 808 666; e-mail: crysdata@fiz-karlsruhe.decrysdata@fiz-karlsruhe.de) on quoting the depository numbers CSD-413778 ($Ce_3Ni_3Si_7$) and CSD-413779 ($La_3Ni_3Si_7$).

4. Elemental analysis

Microprobe analysis on several freshly cleaved crystals of $La_3Ni_3Si_7$ from various batches was performed using a Cameca SX100 electron microscope equipped with a wavelength-dispersive spectrometer. The microprobe was operated at 15 nA beam current at 20 keV accelerating potential. Potential flux inclusions were of particular interest, but no evidence of any other elements besides La, Ni and Si was found. Pure elements were used as standards, and the analysis based on 15 spots (1 μm in size, 30 s counting time) from two different crystals, resulted in a very narrow range of totals—from 99.3(3) to 100.3(3)%. From the data a ratio of La:Ni:Si = 3.00(1):3.07(1):6.95(1) was established, which agrees very well with that refined from single-crystal X-ray data composition (Table 1). This also firmly suggests significant deviation from the previously reported stoichiometry of 3:2:8, and provides a strong argument in support for the presence of mixed Ni/Si site [1,8].

5. Experimental details of the physical property measurements

The dc magnetic susceptibility $\chi \equiv M/H$ measurements were performed by means of a SQUID magnetometer (Quantum Design MPMS-5 model) in fields of 1 kOe in the temperature range 2–350 K. The resistivity was measured with a conventional four-probe method in a home-build He^4-cryostat in the temperature range 1.3–300 K. The current was applied perpendicular to the *b*-axis of the crystals. The specific heat was determined in a He^4 cryostat using thermal relaxation techniques in the temperature range 1.3–20 K. For the temperature range $0.4\,K \leq T \leq 1.5\,K$ the specific heat was measured in a commercial PPMS (Quantum Design).

6. Results and discussion

A schematic representation of the orthorhombic structure of $RE_3Ni_3Si_7$ (RE = La, Ce) is shown in Fig. 1. There are two crystallographically unique RE sites, one Ni site, three Si sites, and one mixed Si + Ni position (M4) in the asymmetric unit of the $RE_3Ni_3Si_7$ structure (Table 2). All of them lie in mirror planes and are in special positions in the space group *Cmmm* (No. 65). Despite the apparent structural complexity and some occupational disorder, all atoms have well-defined atomic displacement parameters. Only the M4 site, which refines as a 50:50 statistical mixture of Si and Ni has slightly elongated thermal parameter (along the *b*-axis). This may suggest that indeed there are only Si–Si and Ni–Ni interactions, which are modeled in the refinement as one statistically

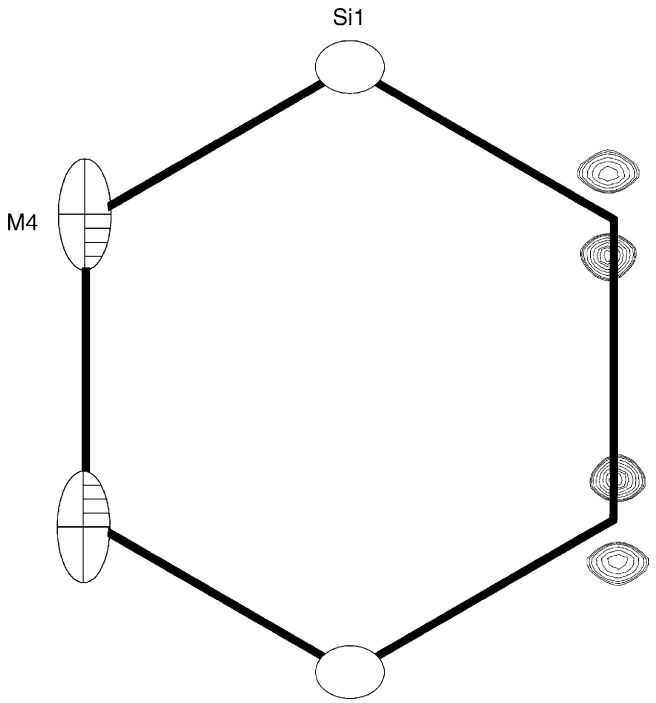

Fig. 2. A fragment of the $RE_3Ni_3Si_7$ structure (thermal ellipsoids are drawn at 98% probability level). The elongation of the M4 thermal parameter along the direction of the *b*-axis is clearly seen. The right hand-site shows slices through the difference Fourier map at $x = 0$, when M4 is refined isotropically.

disordered site. Slices through the difference Fourier map at $x = 0$ when M4 is refined isotropically reveal two well-separated maxima (Fig. 2), which account for the elongation of the thermal ellipsoid in the anisotropic refinement. Similar disorder between Co and Si on one crystallographic site has been reported for $CeCo_{1-x}Si_{2+x}$ [9] with the $CeNiSi_2$-type [10]. This orthorhombic structure is adopted by many intermetallic phases of rare-earths and late transition metals from the Co- and Ni-groups, with Si, Ge and Sn. The majority of these phases are identified from their X-ray powder patterns [11]. However, there are refinement data, including the single-crystal data of the archetype $CeNiSi_2$ [10], which show that one of the Si sites in the structure has considerably smaller thermal parameter—a probable indication for disordered Si/Ni position. The rather complicated $RE_3Ni_3Si_7$ structure could be regarded as an intergrowth between the imaginary structures of $RESi_2$ or rather $RENi_xSi_{2-x}$ (an orthorhombic distortion of the body-centered α-$ThSi_2$ type) and that of $RENi_{2-x}Si_{2+x}$ (orthorhombically distorted $BaAl_4$ type), two common structures types among intermetallic phases that have been extensively studied over the years [12] (Fig. 3).

The corresponding Si–Si and Ni–Si bond distances range from 2.323(1) to 2.437(2) Å. As it can be seen from Fig. 1, the two RE atoms have quite similar coordination environments. RE1 (Wyckoff site 2*a*) lies on three mirror planes, and is situated in the center of a highly symmetric 16-atom polyhedron, built of four Si1, four Si3, and eight M4 atoms (M4

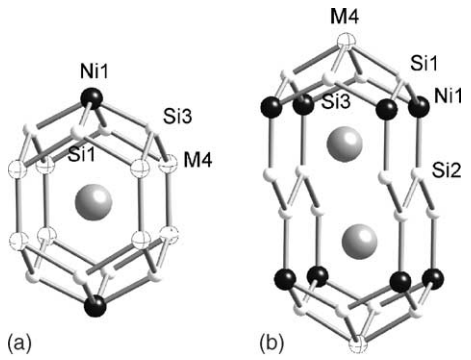

Fig. 3. Coordination environment of RE1 (a), and RE2 (b). The viewing direction is nearly parallel to the *a*-axis.

is refined as disordered Si/Ni, Table 2). The corresponding RE1–Si1 and RE1–Si3 distances are 3.179(2) and 3.226(2) Å, respectively. The RE1–M4 distance is 3.184(7) Å. RE2 coordination polyhedron is similar, although RE2 is in Wyckoff site with symmetry 4f, i.e. with only two mirror planes perpendicular to the *a*- and *c*-axis. RE2 has 14 nearest neighbors (six Si2, two Si3, two Si1, and four Ni1 atoms) at distances ranging from 3.134(2) (RE2–Si3) to 3.229(1) Å (RE2–Ni1). The shortest RE2–RE2 distance is 4.048(1) Å.

Fig. 4 shows the temperature dependence of the magnetic susceptibility of $Ce_3Ni_3Si_7$ measured with the magnetic field along the *b*-axis, i.e. perpendicular to the sample plate, and perpendicular to the *b*-axis, which is parallel to the sample plate. These measurements reveal significant anisotropy. The paramagnetic moments were determined from linear fits of the inverse susceptibility to be $2.60\mu_B$ per Ce-ion for field parallel to the sample plate and $2.44\mu_B$ per Ce-ion for field perpendicular. A polycrystalline average of these values coincides well with the expected value for Ce^{3+} of $2.54\mu_B$. The Weiss temperature θ was calculated to be −21.6 K in the parallel and −140.2 K in the perpendicular measurement. Nega-

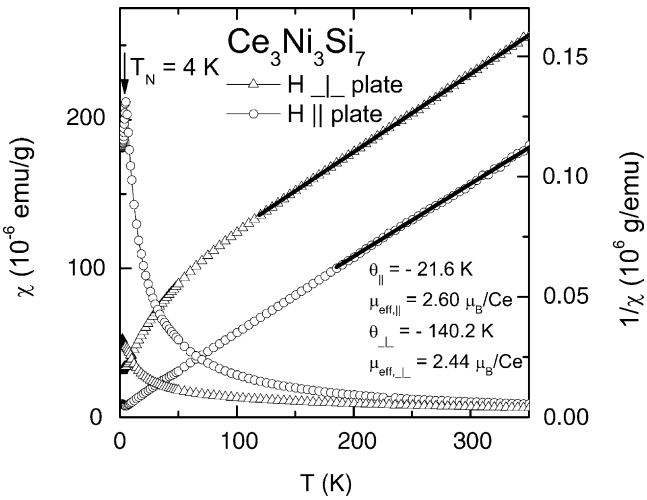

Fig. 4. Susceptibility and inverse susceptibility of $Ce_3Ni_3Si_7$ with the magnetic field parallel (circles) and perpendicular (triangles) to the sample plate. The lines indicate linear fits to determine the paramagnetic moment.

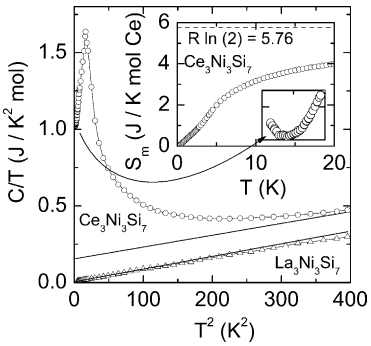

Fig. 5. Specific heat of $Ce_3Ni_3Si_7$ (circles) and $La_3Ni_3Si_7$ (triangles) in the representation C/T vs. T^2. The lines indicate linear fits according to the formula $C/T = \gamma + \beta T^2$. Inset: magnetic entropy of $Ce_3Ni_3Si_7$. Inset in the inset: magnification of the specific heat of $Ce_3Ni_3Si_7$ below $T = 3$ K.

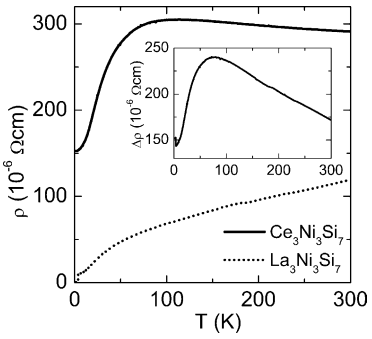

Fig. 6. Resistivity of $Ce_3Ni_3Si_7$ (solid line) and $La_3Ni_3Si_7$ (dotted line); inset: magnetic resistivity of $Ce_3Ni_3Si_7$.

tive Weiss temperatures indicate antiferromagnetic coupling between the Ce-ions. We note that the Weiss temperature is surprisingly high compared to the Néel temperature, even in the polycrystalline average with $\theta \approx 60$ K. Similar behavior was found in $CePd_2Si_2$ ($T_N = 8.5$ K, $\theta = -57$ to -75 K) and $Ce_{0.5}La_{0.5}Pd_2Si_2$ ($T_N = 4$ K, $\theta = -49$ K) [13]. The onset of antiferromagnetic order is clearly observable in the measurement with the field parallel to the sample plate (Fig. 4), the Néel-temperature is $T_N = 4.0$ K, consistent with the results of the specific heat measurement, illustrated in Fig. 5.

To estimate the lattice contribution to the specific heat, we measured $La_3Ni_3Si_7$, which is also shown in Fig. 5. In the chosen representation the specific heat of $La_3Ni_3Si_7$ is a straight line below 14 K, according to the formula $C/T = \gamma + \beta T^2$, where γ represents the electronic contribution and βT^2 the contribution of the lattice. The corresponding fits are indicated as lines in Fig. 5. From these data we estimated the Debye-temperature of $La_3Ni_3Si_7$ to be $\Theta_D = 313$ K and assume the same value for $Ce_3Ni_3Si_7$ because of their nearly equivalent molecular weight. This leads to an electronic specific heat coefficient γ = 51 mJ/K^2 mol Ce extrapolated to $T = 0$ K from above T_N. Noguchi et al. have reported a similar value for γ and a similar Weiss temperature for a polycrystalline sample believed to have the composition $Ce_3Ni_2Si_8$, i.e. $x = 0$. Our results suggest that the composition of their sample probably is closer to $x = 1$.

From the magnetic part of the specific heat $C_m/T = C/T(Ce_3Ni_3Si_7) - C/T(La_3Ni_3Si_7)$ we calculated the magnetic entropy, which is drawn in the inset of Fig. 5. The theoretical value of 5.76 J/mol K for a $S = 1/2$-system is indicated by the dashed line. At the Néel-temperature only 27% of this value is reached and the entropy saturates with only 69% of the expected value. These values are reasonable, taking into account the Kondo-effect present in the sample. Additionally, there is an upturn in C/T below 1.5 K. This may suggest that the crystallographically inequivalent Ce ions order separately at 4 K and at some temperature below 1.5 K. Measurements to lower temperatures would be useful in clarifying this issue.

Finally, we discuss the electrical resistivity, which is presented in the upper frame of Fig. 6. Starting from room temperature the electrical resistivity of $Ce_3Ni_3Si_7$ increases slightly with decreasing temperature. It reaches a maximum at 115 K and falls steeply below this temperature. Below 3 K the resistivity saturates. The residual resistance ratio $RRR = 1.91$, together with the absolute value of the resistivity at room temperature $\rho(300\,\text{K}) \approx 300\,\mu\Omega\,\text{cm}$ confirms the sample to be a poor metal. Noguchi et al. reported a semiconducting characteristic for the resistivity of their sample [8], probably due to enhanced contact resistances at the grain boundaries.

The resistivity of $La_3Ni_3Si_7$ shows a positive temperature gradient over the entire temperature range. At $T_C = 3.7$ K a superconducting transition due to Sn flux is observed. The RRR (above the superconducting transition) is 11.8, more than one order of magnitude higher than in the Ce-compound. The improved conductivity of $La_3Ni_3Si_7$ can be explained by the lack of magnetic scattering centers in that non-magnetic sample. This is reflected in the high absolute values of the magnetic part of the resistivity of $Ce_3Ni_3Si_7$, which we obtained by subtracting the resistivity of the La-compound from the resistivity of the Ce-compound. The result is drawn in the inset of Fig. 6. The maximum is shifted down to $T^* = 75$ K. This maximum can be attributed to the Kondo effect, i.e. additional scattering of the conduction electrons by the magnetic $4f$-ions. This is supported by calculating the Sommerfeld coefficient from the Kondo temperature T^*, using the expression for a single impurity Kondo system $\gamma = (\nu - 1)\pi R/(6T^*) = 58$ mJ/K^2 mol Ce, where $\nu = 2J + 1$ [14]. The result coincides fairly with $\gamma = 51$ mJ/K^2 mol Ce obtained from the specific heat measurements.

The question arising from this data is can $Ce_3Ni_3Si_7$ be described as a heavy fermion system. For a heavy-fermion system the value of the Sommerfeld-coefficient γ is relatively small. On the other hand, the results of resistivity and specific heat, from which the entropy was calculated, indicate the presence of the Kondo-effect. As pointed out in [15]. the occurrence of magnetic order in a Kondo-system reduces γ significantly. Thus, the description of $Ce_3Ni_3Si_7$ seems to be justified in spite of the moderate value of γ.

7. Conclusion

We investigated the structural and magnetic properties of $Ce_3Ni_3Si_7$, using X-ray diffraction, magnetic susceptibility, specific heat and electrical resistivity measurements. X-ray diffraction and elemental analysis reveal that the composition of this compound is $Ce_3Ni_{2+x}Si_{8-x}$ with $x \approx 1$, with some Ni-atoms occupying Si-sites. Our single-crystal work clarifies and corrects the older studies [1] and the refinement, together with the elemental analysis, suggests that the compound should be reformulated as $Ce_3Ni_3Si_7$. The susceptibility shows Curie-Weiss behavior above 200 K, with an effective magnetic moment corresponding to the expected moment for Ce^{3+}. The onset of antiferromagnetic order at T_N is confirmed by specific heat measurements. The Sommerfeld-coefficient, obtained from the specific heat coincides fairly with the Kondo temperature T^*, determined from the electrical resistivity. In summary, $Ce_3Ni_3Si_7$ is a very light heavy-fermion system with antiferromagnetic order at $T_N = 4$ K and possibly below 2 K.

Acknowledgements

The work was performed under the auspices of the U.S. Department of Energy. S. Bobev acknowledges support from I.C.A.M.

References

[1] J.A. Stepien, K. Lukaszewicz, E.I. Hladyszewski, O. Bodak, Crystalline structure of the intermetallic compound $Ce_3Ni_2Si_8$, Bulletin de l'Académie Polonaise des Sciences 20 (11–12) (1972) 1029–1036.
[2] P.C. Canfield, Z. Fisk, Growth of single-crystals from metallic fluxes, Phil. Mag. B 65 (6) (1992) 1117–1123.
[3] Bruker Analytical X-ray Systems Inc., Madison WI, SMART NT Version 5.05, 1998.
[4] Bruker Analytical X-ray Systems Inc., Madison WI, SAINT NT Version 6.22, 1998.
[5] Bruker Analytical X-ray Systems Inc., Madison WI, SADABS NT Version 2.05, 1998.
[6] Bruker Analytical X-ray Systems Inc., Madison WI, SHELXTL Version 5.10, 1997.
[7] A.J.C. Wilson, E. Prince (Eds.), International Tables for Crystallography, vol. C, 6th ed., Kluwer Academic Publishers, Norwell, MA, 1999, p. 548.
[8] S. Noguchi, K. Okuda, H. Nojiri, M. Motokawa, Magnetic properties of $Ce_3Ni_2Si_8$, Physica B 281 (2000) 79–80.
[9] B. Chabot, E. Parth, J. Steinmetz, Single-crystal studies of non-stoichiometric $CeNiSi_2$-type phases in the Ce-Co–Si and Lu-Co–Si systems, J. Less-Common Met. 125 (1986) 147–156.
[10] O.I. Bodak, E.I. Gladishevskii, The crystal structure of $CeNiSi_2$ and related compounds, Kristallogr 14 (1969) 990–994.
[11] P. Villars, L.D. Calvert (Eds.), Pearson's Handbook of Crystallographic Data for Intermetallic Compounds, 2nd ed., American Society for Metals, Materials Park, OH, 1991.
[12] A. Szytula, J. Leciejewicz (Eds.), Handbook of Crystal Structures and Magnetic Properties of Rare Earth Intermetallics, CRC Press, Boca Raton, FL, 1994 .
[13] R.A. Steeman, T. Endstra, S.A.M. Mentink, E. Frikkee, A.A. Menovsky, G.J. Niewuwenhuys, J.A. Mydosh, Magnetic properties of $Ce_{0.5}La_{0.5}Pd_2Si_2$, Physica B 163 (1990) 597–599.
[14] V.T. Rajan, Magnetic susceptibility and specific heat of the coqblin-schrieffer model, Phys. Rev. Lett. 51 4 (1983) 308–311.
[15] Z. Fisk, J.D. Thompson, H.R. Ott, Heavy-electrons: new materials, J. Magn. Magn. Mater. 76–77 (1988) 637–641.